Variation of electronic structure in $La_{1-x}Sr_xMnO_3$ $(0 \leqslant x \leqslant 0.3)$ as investigated by optical conductivity spectra

Y. Okimoto, T. Katsufuji, T. Ishikawa, T. Arima,* and Y. Tokura
Department of Applied Physics, University of Tokyo, Tokyo 113, Japan
(Received 30 September 1996)

Optical conductivity spectra and their variation with temperature and doping level x have been investigated for single crystals of $La_{1-x}Sr_xMnO_3$ $(0 \leqslant x \leqslant 0.3)$. For the low-doped insulating crystal $(x=0.1)$ which shows a ferromagnetic insulating state at low temperature, the spectral weight of the optical conductivity increases only in the inner-gap region around 0.5 eV, but no Drude part emerges due to carrier localization effect. For $x \geqslant 0.17$, where the low-temperature ferromagnetic metallic state shows up, the optical conductivity spectrum above T_c is characterized by interband transitions between the exchange-split conduction bands, and it gradually changes into that of intraband excitations below T_c. The energy scale (up to ≈ 2 eV) of the spectral weight transfer is determined by the effective Hund's-rule coupling energy. In the metallic phase, low-energy spectra arising from intraband excitations can be sorted into two parts: One is a nearly ω-independent broad structure (incoherent part), and the other a sharp coherent Drude peak with anomalously low spectral weight. This can hardly be reconciled with the simple double-exchange theory, but indicates that another degree of freedom (e.g., the orbital ordering and/or electron-lattice interactions) should be taken into account. [S0163-1829(97)11707-6]

I. INTRODUCTION

Hole-doped manganese oxides with perovskite-type structure have long been known as one of prototypical conducting ferromagnets.[1–3] The ferromagnetic metallic state in these compounds is stabilized by the double-exchange mechanism[4–6] originating from the strong coupling between the charge-carriers and local spins which are both dominantly of the $3d$ orbital character. In the course of the recent renaissance of study on the $3d$ transition-metal oxides, these double-exchange systems have been revisited, and their interesting aspects are being unraveled. Those are versatile intriguing phenomena induced by a magnetic field, such as ''colossal'' magnetoresistance observed commonly near the ferromagnetic transition temperature (T_c) in the most of the doped manganites,[7–14] the field-melting of the charge- and/or orbital-ordered state accompanying a huge change of the resistivity,[15–18] and field-induced structural transitions even near room temperature,[19,20] field control of intergrain or interplane tunneling of highly spin-polarized carriers,[21,22] and so on. All these phenomena are considered as relevant to unique electronic structures of the perovskite-type manganites in which mutual coupling among the charge, spin, orbital and lattice degrees of freedom is particularly important. In this paper, we adopt crystals of $La_{1-x}Sr_xMnO_3$ as the most prototypical double-exchange system, and investigate anomalously large variation of their electronic structures with temperature and hole-doping level (x) by measurements of optical conductivity spectra.

The parent material $LaMnO_3$ is a charge-transfer type (CT-type) insulator[23,24] in the Zaanen-Sawatzky-Allen scheme,[25] and has four d electrons per Mn^{3+} site with a configuration of $t_{2g}^3 e_g^1$. As the nominal hole concentration (x) is increased, $La_{1-x}Sr_xMnO_3$ shows a phase change from an antiferromagnetic to ferromagnetic state around $x=0.1$, and subsequently the low-temperature ferromagnetic phase undergoes an insulator-to-metal transition around $x=0.17$.[1,3,10] Such a conducting ferromagnetic state is explained by the double-exchange mechanism.[4–6] In the metallic phase, the conduction band consists of $3de_g$ state hybridized strongly with the O $2p$ state, while the t_{2g} electrons are still localized, forming local spins $(S=\frac{3}{2})$. The strong interaction (Hund's-rule coupling) between an e_g electron and a t_{2g} local spin plays an important role in the electronic properties of this system.

As a model in the doped manganites, Kubo and Ohata[26] proposed the following Kondo lattice model with ferromagnetic exchange coupling $(J_H>0)$:

$$H=-\sum_{i,j,\sigma} t_{i,j}(c_{i,\sigma}^{\dagger}c_{j,\sigma}+\text{H.c.})-J_H\sum_i \vec{s}_i\cdot\vec{S}_i . \qquad (1)$$

Here $\vec{s}_i$ represents the spin of the itinerant e_g electron, and $\vec{S}_i$ the localized t_{2g} spin $(S=\frac{3}{2})$. The Hund's-rule coupling energy SJ_H [≈ 2 eV (Ref. 23)] exceeds the one-electron bandwidth (W).[27] A consequence of this strong electron-spin coupling is the exchange-splitting of the spin-polarized conduction bands by $\approx SJ_H$ and the spin-polarization of the conduction electrons varies from 0 to 100% with lowering temperature. Recently, Furukawa[28,29] derived the optical conductivity from this Kondo lattice model by the dynamical mean-field approximation, and showed that the spectra are critically dependent on the spin-polarization accompanying the spectral weight transfer from the interband transitions between the exchange-split bands to the Drude part. Therefore, the optical spectroscopy in the photon energy region up to above $\approx SJ_H$ is indispensable to clarify the spin-polarization dependent electronic features in $La_{1-x}Sr_xMnO_3$.

Among a number of compositional combinations, the $La_{1-x}Sr_xMnO_3$ system is most appropriate for a first-stage spectroscopic investigation in the sense that it is relatively less affected by other instabilities, such as electron-lattice or charge- and/or orbital-ordering interactions. This is because the W value of the $La_{1-x}Sr_xMnO_3$ system is the largest among various perovskite-type manganites due to the minimal or no orthorhombic lattice distortion.[14] Nevertheless, we will show several anomalous features in the low-energy optical conductivity spectra of this system which can be hardly reconciled in terms of the simple double-exchange model as described by Eq. (1).

A part of the results for the specific hole concentration ($x=0.175$) has been published in a form of short letter.[30] In this paper, we present full results of the spectra of $La_{1-x}Sr_xMnO_3$ ($x=0.1$, 0.175, and 0.3) together with the discussion on the variation of electronic structures with spin-polarization (temperature) as well as with the nominal hole concentration x.

II. EXPERIMENT

A. Sample preparation and characterization

All the crystals investigated were single crystals melt grown by a floating zone method as described in detail in Ref. 14. Measurements of powder x-ray-diffraction patterns showed that all the obtained samples were of single phase, and that the crystal structure at room temperature were orthorhombic ($x=0$, 0.1, and 0.175) and rhombohedral ($x=0.3$). Analyses of chemical composition were performed for each sample using an electron probe microanalyzer and redox titration, and showed the almost identical composition with the prescribed ratio.[14] To characterize the compounds, we measured the temperature dependence of the resistivity and the magnetic susceptibility. For the resistivity measurements, the samples were cut to a rectangular shape, and a standard four-probe technique was used. Magnetic susceptibility was measured with a superconducting quantum interference device magnetometer.

To overview the electronic behaviors of the manganites to which we have measured optical spectra, in Fig. 1 we show the temperature dependence of resistivity (ρ) in $La_{1-x}Sr_xMnO_3$ ($x=0$, 0.1, 0.175, and 0.3) together with the electronic phase diagram. $LaMnO_3$ ($x=0$) is a correlated insulator with a layer-type (A-type) antiferromagnetic spin structure.[31,32] As the nominal hole concentration x increases, the ferromagnetic phase shows up and the Curie temperature T_c increases as indicated in the resistivity curve (the lower panel of Fig. 1) by arrows. In the region of $x\geqslant 0.1$, cusp structures appear in the ρ-T curve around T_c. At $x=0.1$, the ρ-T curve shows an insulating behavior ($d\rho/dT<0$) apart from the temperature region immediately below T_c, and most of the ferromagnetic phase[33] remains insulating. By contrast, the resistivity for $x\geqslant 0.17$ shows a metallic behavior ($d\rho/dT>0$) below T_c. The resistivity of the metallic state at the lowest temperature is two orders of magnitude smaller than that around T_c. There is a difference between $x=0.175$ and $x=0.3$ in the resistivity above T_c. The $x=0.175$ crystal shows a semiconducting ($d\rho/dT<0$) behavior above T_c, which is perhaps due to the combination effect of the spin scattering in the paramagnetic state and some random potential scattering[34] or dynamic Jahn-Teller coupling.[35] For $x=0.3$, however, the ρ-T curve shows a metallic behavior over the whole temperature region.

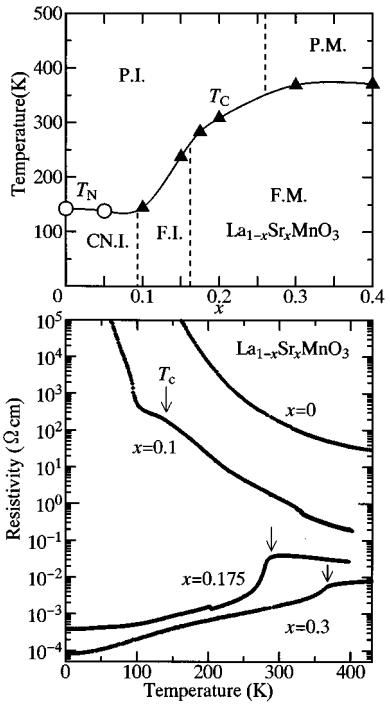

FIG. 1. Upper panel: Electronic phase diagram of $La_{1-x}Sr_xMnO_3$ after Urushibara *et al.* (Ref. 14): P.I. (paramagnetic insulator), CN.I. (spin-canted insulator), F.I. (ferromagnetic insulator), P.M. (paramagnetic metal), and F.M. (ferromagnetic metal). Lower panel: Temperature dependence of resistivity in crystals of $La_{1-x}Sr_xMnO_3$ ($x=0$, 0.1, 0.175, and 0.3), for which the optical spectra were measured. Arrows indicate the respective Curie temperature T_c.

B. Optical measurements

Reflectivity spectra of near-normal incidence were measured for crystals of $La_{1-x}Sr_xMnO_3$ ($x=0$, 0.1, 0.175, and 0.3) with a typical size of $\approx 6\times 6\times 1$ mm^3. Reflectivity spectra in the far- and mid-infrared range 0.01–0.8 eV were measured using a Fourier transform type interferometer with a 4.2-K bolometer (0.01–0.1 eV) and MCT detector (0.08–0.8 eV). Grating-type monochromators were used for the higher-energy range, 0.6–36 eV. For the measurement above 6 eV, we made use of synchrotron radiation at the Institute for Solid State Physics, University of Tokyo. In order to investigate the temperature dependence of the optical spectra, we measured reflectivity spectra at selected temperatures up to 3.0 eV. As a reference mirror, we used evaporated Au film (far- or near-infrared region), and Ag film (visible range). We fixed the reference mirror near the sample within a cryostat and interchanged with the sample. That is, all the spectra were measured at each temperature from 0.01 to 3 eV, and extrapolated by the data above 3 eV at room temperature. Such a procedure is possible and reasonable because the variation of the reflectivity in the high-energy region with the change of the temperature is negligibly small (less than 1% at 3.0 eV).

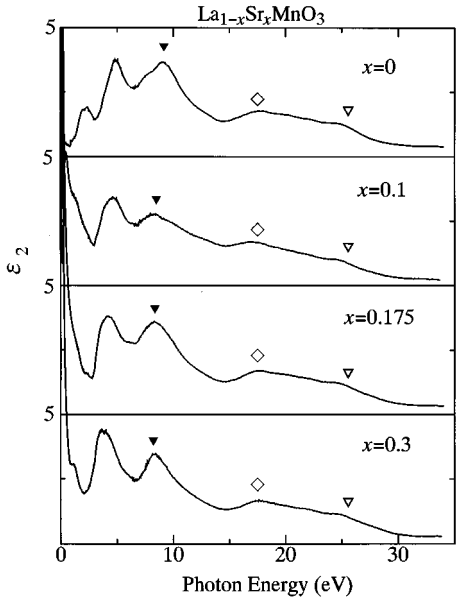

FIG. 2. ϵ_2 (imaginary part of dielectric constant) spectra in $La_{1-x}Sr_xMnO_3$ ($x=0.1$, 0.175, and 0.3) at 9 K. (The spectra above 3.0 eV were measured at room temperature, and connected to these at 9 K.)

The optical conductivity spectra were obtained by Kramers-Kronig analysis of the reflectivity data. For this analysis, we assumed the constant reflectivity below 0.01 eV for all the data. It was confirmed that the optical conductivity spectra above 0.01 eV were not sensitive to the extrapolation procedure. For higher-energy reflectivity than 36 eV, ω^{-4}-type extrapolation was used.

III. OVERALL FEATURES OF OPTICAL SPECTRA

First, let us overview the optical spectra of $La_{1-x}Sr_xMnO_3$ in a wide photon energy region. Arima and Tokura[36] have recently investigated the optical spectra of a series of $LaMO_3$ (M being $3d$ transition-metal elements), and revealed the character of optical transitions in the respective spectra. In the following, we refer to their assignments for the interpretation of the higher-lying transitions in $La_{1-x}Sr_xMnO_3$.

In Fig. 2 we show the ϵ_2 spectra deduced by Kramers-Kronig analysis. As for the structures above 6 eV, there are three major peaks around 25, 17, and 8 eV in the ϵ_2 spectra for all the x values. The $\approx$25-eV structure marked with open triangles can be assigned to the intra-atomic transition between La $5p$ and $5d$. This transition was observed to show a systematic variation with the rare-earth element R, as observed in other perovskite series, $RNiO_3$ (Ref. 36) and $RCoO_3$.[37] The structures around 17 (open squares) and 8 eV (closed triangles) correspond to interband transitions from O $2s$ to Mn $3d$ and from O $2p$ to La $5d$, respectively.[36] These assignments are consistent with those based on the photoemission and x-ray (O $1s$) absorption spectra of $La_{1-x}Sr_xMnO_3$ by Saitoh *et al.*[24] In contrast to these x-independent features of higher-lying (>8 eV) transitions, the lower-energy part of ϵ_2 shows a large variation with the hole concentration x.

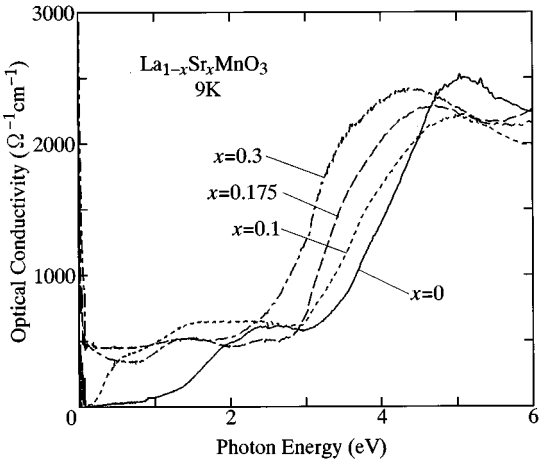

FIG. 3. Optical conductivity spectra in $La_{1-x}Sr_xMnO_3$ ($x=0.1$, 0.175, and 0.3) at 9 K. (The original reflectivity spectra above 3.0 eV, being nearly independent of temperature, were measured at room temperature, and connected to those at 9 K. See text.)

To scrutinize the changes in the lower-lying transitions, we show in Fig. 3 the optical conductivity spectra ($\sigma(\omega)$) at 9 K in $La_{1-x}Sr_xMnO_3$ ($x=0-0.3$) in the photon energy region of 0–6 eV. The 9-K spectra are viewed as representing the ground-state feature for the respective doping (x) levels. The $\sigma(\omega)$ spectrum of the end insulator $LaMnO_3$ (a solid line) has two notable optical excitations around $\approx$1.7 and $\approx$3.0 eV. The shape of the spectrum nearly agrees with that measured by Arima and coworkers at room temperature.[23,36] They assigned these structures to CT gap excitations, $t_{2g}^3e_g^1 \rightarrow t_{2g}^3e_g^2\underline{L}$ (the lower-energy band) and $t_{2g}^3e_g^1 \rightarrow t_{2g}^4e_g^1\underline{L}$ (the higher-energy one), and estimated the Hund's-rule coupling energy J_H between an e_g electron and a t_{2g} spin ($SJ_H \approx 2$ eV).[36] The onset of the second CT excitation shifts to a lower energy as x increases. This is because the occupied O $2p$ states shift upward in energy due to the change of the Madelung-type electrostatic potential in the Sr-substituted lattice.[38] Similar effects are also observed in other transition metal oxides, e.g., $Y_{1-x}Ca_xTiO_3$ (Ref. 39) and $La_{1-x}Sr_xVO_3$.[40] The lower-energy part in $\sigma(\omega)$ forms a gap structure for $x=0$ with the onset of $\sigma(\omega)$ (the first CT excitation) around 1.2 eV. With hole-doping ($x \neq 0$), the gap appears to be filled in, in accord with the phase change into the metallic state. However, the spectral shape of $\sigma(\omega)$ in the metallic phase ($x \geqslant 0.17$) seems to be unconventional, being far from a simple Drude type even as compared with other carrier-doped $3d$ transition-metal oxides.[39,41,42] We will come back to this problem in Sec. IV B.

IV. SPECTRAL WEIGHT TRANSFER WITH SPIN POLARIZATION

A. Temperature- and doping (x) dependence of optical conductivity spectra

In Fig. 4 we show reflectivity spectra for $x=0.1$, 0.175, and 0.3 with varying temperature from above T_c down to 9 K. The reflectivity spectra for $x=0.1$ [Fig. 4(a)] show an insulating behavior: There are more than three spiky structures in the infrared region due to the optical-phonon modes.

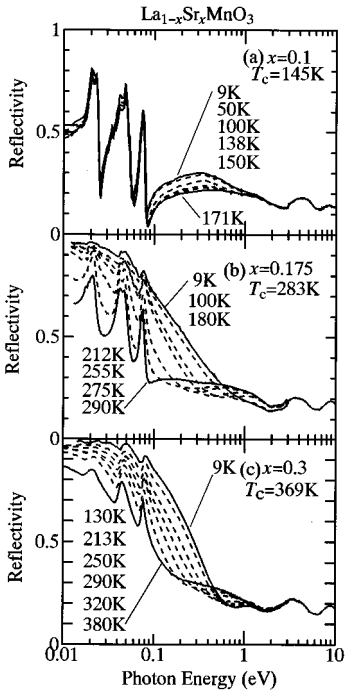

FIG. 4. Reflectivity spectra at various temperatures in $La_{1-x}Sr_xMnO_3$: (a) $x=0.1$, (b) $x=0.175$, and (c) $x=0.3$.

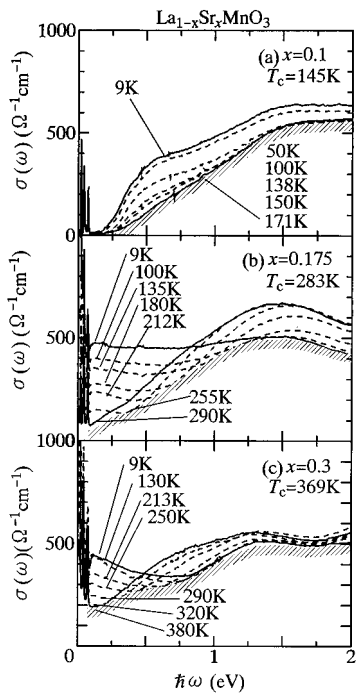

FIG. 5. Optical conductivity spectra at various temperatures in $La_{1-x}Sr_xMnO_3$: (a) $x=0.1$, (b) $x=0.175$, and (c) $x=0.3$. The hatched curves represent the temperature-independent parts of the spectra deduced from the envelope of the respective curves.

With a decrease of temperature the reflectivity around 0.3 eV gradually increases, but little change occurs in the far-infrared region below 0.06 eV. On the contrary, the spectra for $x=0.175$ [Fig. 4(b)] and 0.3 [Fig. 4(c)] show a large variation with temperature. For both compositions, the respective spectra above T_c seem to be rather characteristic of insulators with distinct optical-phonon structures, but with a decrease of temperature the low-energy part of the reflectivity spectra evolves and finally turns into a metallic high-reflectivity band.

To investigate the electronic structure quantitatively, we derived optical conductivity spectra $\sigma(\omega)$ by Kramers-Kronig analysis. In Fig. 5 we show the temperature dependence of $\sigma(\omega)$ for $x=0.1$, 0.175, and 0.3. In the $x=0.1$ spectra [Fig. 5(a)], there is little spectral weight below 0.2 eV apart from that of the three major phonon modes. As temperature decreases, the spectral weight is gradually accumulated in the mid-infrared region around 0.3 eV, but never transferred down to the low-energy region below 0.1 eV. This is in accord with the carrier localization behavior as seen in the ρ-T curve for $x=0.1$ (Fig. 1). In the $\sigma(\omega)$ spectra for the $x=0.175$ [Fig. 5(b)] and 0.3 [Fig. 5(c)], on the other hand, the spectral weight shows a large temperature-dependent variation up to above 2 eV, indicating that the quantity that governs the spin-polarization-dependent electronic structure has a large energy scale. In Figs. 5(b) and 5(c), each spectrum above T_c (with no spin polarization) forms a broad peak (at $\approx$1.5 eV for $x=0.175$ and $\approx$1.3 eV for $x=0.3$). These broad peaks are mainly composed of the interband transitions between the O $2p$ and Mn $3d$ (e_g) states, but their spectral weight gradually decreases and is transferred into the lower-energy part, 0–1.0 eV for $x=0.175$ and 0–0.5 eV for $x=0.3$, with decrease of temperature. It is noteworthy that there is a clear difference in the energy scale of the spectral weight transfer between $x=0.175$ and 0.3. Such a temperature dependence of $\sigma(\omega)$ over a wide photon energy region is quite unconventional, and reminiscent of the Mott transition in the correlated electron system.

To analyze the spectral weight transfer with change of temperature (or spin polarization of the conduction electrons), we extract the temperature-independent part from the optical conductivity spectra. In Figs. 5(a)–5(c), the respective curves of $\sigma(\omega)$ spectra at various temperatures form an envelope as depicted by a hatched curve in the figure which is composed of the lowest-lying points of all the conductivity spectra at each photon energy. It is reasonable to consider that such a temperature-independent part stands for the ''background'' interband transitions between the O $2p$ and Mn $3d$ band which are not affected by change of spin polarization. Here we define a reduced optical conductivity spectrum ($\tilde{\sigma}(\omega)$) by subtracting the temperature-independent part (drawn by hatching) from each $\sigma(\omega)$ spectrum. In Figs. 6(a), 6(b), and 6(c), we show $\tilde{\sigma}(\omega)$ spectra for $x=0.1$, 0.175, and 0.3, respectively. We omitted the infrared phonon parts to avoid complexity. In Fig. 6(a) ($x=0.1$), the spectral weight in the midinfrared region increases with decrease of the temperature. On the other hand, Figs. 6(b) and 6(c) ($x=0.175$ and 0.3) show that the gaplike transition on the higher-energy side above T_c is gradually reduced in intensity, and changes into the $\omega=0$ centered band as temperature decreases.

The formation of a midinfrared peak as observed in the low-temperature $\tilde{\sigma}(\omega)$ spectra for $x=0.1$ is often seen in the spectra of low-doped Mott-insulators which still remain insulating or semiconducting due to some localization

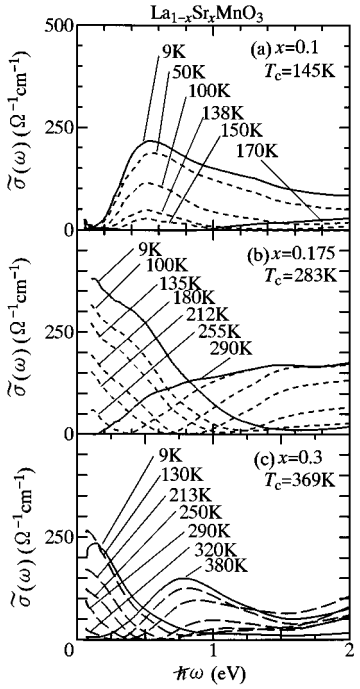

FIG. 6. Reduced optical conductivity spectra which are derived by subtracting the temperature independent part (the hatched curves in Fig. 5) at various temperatures in $La_{1-x}Sr_xMnO_3$: (a) $x=0.1$, (b) $x=0.175$, and (c) $x=0.3$. The far-infrared region dominated by the optical phonons is omitted to avoid complexity.

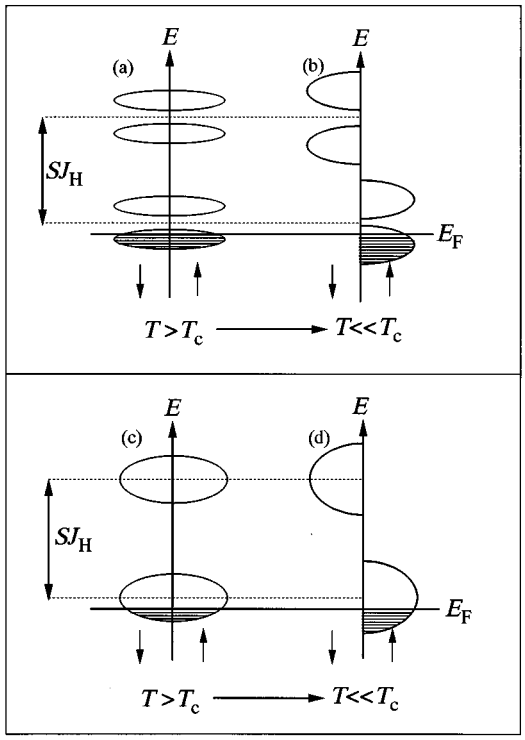

FIG. 7. Schematics for the variation of the spin-polarized conduction e_g bands with temperature in the double-exchange manganites in the presence [upper panel, (a) and (b)] and absence [lower panel, (c) and (d)] of Jahn-Teller distortions.

effect.[40,41,43,42] In general, such a midinfrared peak eventually shifts to lower energy, forming an $\omega=0$ centered peak (a quasi-Drude band) upon the insulator-metal transition with further doping. The observed change of the ground state $\tilde{\sigma}(\omega)$ spectra in going from $x=0.1$ to 0.175 [see and compare the 9-K $\tilde{\sigma}(\omega)$ spectra shown in Fig. 6] is consistent with this general tendency. The localization of doped carriers in the $x=0.1$ manganite is likely to come from the Jahn-Teller (JT)-type electron-lattice coupling (formation of JT polarons) (Refs. 44 and 45) in addition to the conventional random potential effect due to the alloying of the (La,Sr) site. In this case, the spin-polarized e_g conduction bands are subject to the splitting (Δ_{JT}) due to the JT distortion, as schematically shown in Fig. 7(b), as well as in the paramagnetic case [Fig. 7(a)]. Then the lower-lying $\tilde{\sigma}(\omega)$ band has a character of the interband transitions between the JT-split up-spin bands. The growth of the spin polarization with decrease of temperature should tend to increase the spectral intensity because of the effective increase in the e_g electron transfer interaction. The feature is in accord with the observed result, and also clearly demonstrated by the dynamical mean-field calculation for the strong JT-coupling case by Millis, Mueller, and Shraiman,[44] who took into account both double-exchange and JT interactions. The band peak energy ($\approx$0.5 eV) observed in the $x=0.1$ spectra thus gives a measure of the binding energy (Δ_{JT}) of the JT polaron.

The spin-polarization-dependent change in $\tilde{\sigma}(\omega)$ for the ferromagnetic metallic phase ($x=0.175$ and 0.3) may be interpreted more straightforwardly in terms of the simple double-exchange model,[28,30] since the JT coupling effect is less important for the higher-x metallic phase. As shown in the lower panel of Fig. 7, the Hund's-rule coupling energy SJ_H (S being the magnitude of the t_{2g} local spin) between the e_g conduction carriers and t_{2g} local spins ($S=\frac{3}{2}$) perhaps exceeds the one-electron bandwidth (W) of e_g electrons.[27] Under this circumstance ($SJ_H>W$), the e_g band should split into two bands by SJ_H, as shown in Figs. 7(c) and 7(d).[28,29] Above T_c, such exchange-split bands are equally composed of two subbands, i.e., an up-spin band and a down-spin band. Optical transitions are allowed only between the lower and upper up- (or down-) spin bands. A gaplike feature in $\tilde{\sigma}(\omega)$ spectra above T_c is thus assigned to the interband transition between the exchange-split bands.

As temperature is decreased below T_c, the density of states (DOS) for the respective subbands is modified in a spin dependent manner: The DOS for the lower (upper) up-spin band increases (decreases), whereas that for the lower (upper) down-spin band decreases (increases) with an increase of the net magnetization. At $T=0$, the exchange-split bands turn into two completely spin-polarized bands, between which the optical transitions are forbidden. Therefore, the spectral weight of the *interband* transitions between the exchange-split bands is decreased, while that of the *intraband* excitation within the lower up-spin band gradually grows up. The spectral weight transfer with decrease of temperature as seen in Figs. 6(b) and 6(c) can be interpreted as from the interband transitions to the intraband ones. Such an unconventional variation of the optical spectra with spin polarization (or with temperature) thus arises from the strong spin (t_{2g}) electron (e_g) coupling ($SJ_H>W$) characteristic of the doped manganite system.

Keeping the above in mind, let us see in more detail the T- and x-dependent changes in $\tilde{\sigma}(\omega)$ spectra for the metallic

$x=0.175$ and $x=0.3$ crystals. As clearly seen in Fig. 6, the energy scale of the spectral weight transfer is decreasing with hole doping. The peak energy of the upper exchange-split band in $\tilde{\sigma}(\omega)$ should approximately correspond to SJ_H [in the definition of J_H by Eq. (1)].[29] For $x=0.175$, $SJ_H \approx 2$ eV, which is consistent with the estimate based on the optical spectrum of $LaMnO_3$.[36] But the effective value of SJ_H is estimated as ≈ 0.9 eV for $x=0.3$ by taking the peak position of the interband transitions in the $\tilde{\sigma}(\omega)$ spectrum, and is considerably smaller than that for $x=0.175$. This means that spin-charge coupling strength as measured by SJ_H/W decreases as the hole concentration x is increased. The present spectroscopic results directly indicate the crossover from the strong-coupling to the medium- or weak-coupling regime with hole doping. The origin of the variation of the effective J_H value with x may be explained as follows: We have so far assumed that the spin-polarized conduction bands are of $3d\ e_g$ orbital character. However, this picture is too simple for a quantitative argument of the electronic structure, and the p-hole character has to be taken into account. In fact, the parent compound $LaMnO_3$ should rather be sorted into the charge-transfer insulator than the Mott-Hubbard insulator in the Zaanen-Sawatzky-Allen scheme, and the doped hole should be in the strongly d-p hybridized state, as shown by photoemission spectroscopy.[24] The larger admixture of the p-hole character then tends to reduce the effective exchange splitting, since the effective antiferromagnetic exchange coupling between the Mn local spin ($S=2$) and p-hole spin is mediated by the second-order process and should be much reduced as compared with the bare J_H value. As shown by a fairly large (by ≈ 1 eV) red-shift of the 4-eV charge-transfer band shown in Fig. 3, the Sr doping up-shifts the O $2p$ state in general, and increases the O $2p$ hole character for the conduction band. Thus, the effective exchange splitting of the spin-polarized conduction band is nominally screened and reduced with hole doping x, even though the bare J_H value is least changed by hole doping.

B. Coherent versus incoherent part in low-energy part of optical spectra

In Fig. 8 we show a magnification of $\sigma(\omega)$ for $x=0.175$ in the low-energy region. With a decrease in temperature, the conductivity at 0.05–0.1 eV is increased nearly independently of photon energy. By contrast, the 9-K spectrum below 0.05 eV steeply increases with a decrease in photon energy, indicating the presence of a Drude peak characteristic of the metallic state. The value of dc conductivity $\sigma(0)$ at 9 K is $2.6\times10^3\ \Omega^{-1}\mathrm{cm}^{-1}$ (see Fig. 1), and comparable to that obtained by extrapolating the $\sigma(\omega)$ spectrum.

Such a Drude part is observed notably as well in the $\sigma(\omega)$ spectra of $x=0.3$, as shown in Figs. 9(a) and 9(b). As the temperature is decreased, the conductivity is at first increased below 0.1 eV from 380 to 130 K [see Fig. 9(a)], but decreased when the temperature is further lowered below 130 K [see Fig. 9(b)]. The observed spectral change reminds us of the infrared feature of the c-axis spectra of the cuprate superconductors in which $\sigma(\omega)$ is suppressed with decrease of temperature giving rise to a δ-function peak below T_c.[46] The value of the dc conductivity from the resistivity measurements [$\sigma(0)\approx10^4\ \Omega^{-1}\mathrm{cm}^{-1}$ at 9 K] is much larger than the value of $\sigma(\omega)$ at $\omega=0.01$ eV, the smallest energy in the present spectra. The major spectral weight of the coherent part is likely to lie in even a lower-energy region than the one displayed here.

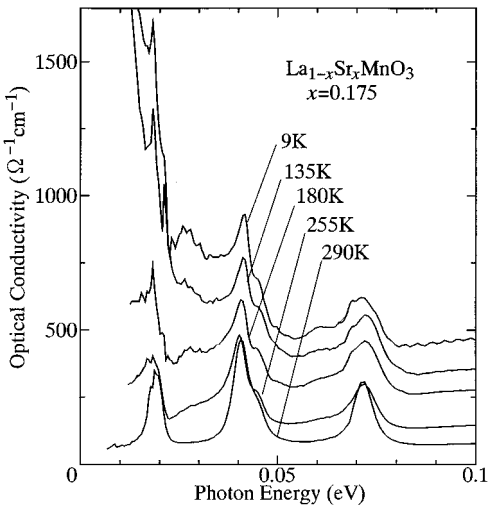

FIG. 8. Low-energy parts of the optical conductivity spectra in $La_{1-x}Sr_xMnO_3$ ($x=0.175$) at various temperatures.

The Drude weight was estimated by the fitting procedure with use of the dielectric function of Drude form plus Lorentz oscillators,[47]

$$\tilde{\varepsilon}=\varepsilon_\infty-\frac{\omega_p^2}{\omega^2+i\omega\Gamma_D}+\sum_j\frac{S_j}{\omega_j^2-\omega^2+i\omega\Gamma_j}. \qquad (2)$$

As for the Drude form, we adopt the dc conductivity (cf. Fig. 1) as the $\sigma(\omega\rightarrow0)$ value, and hence the fitting parameter is the scattering rate, Γ_D. We exemplify in Fig. 10 the result of fitting for the $x=0.175$ crystal at 9 K. The calculated curve shown by a solid line reproduces the experimental spectrum (open circles). Among the decomposed components used in the fitting procedure, the Drude (coherent) and incoherent parts are displayed by dotted and dashed lines,

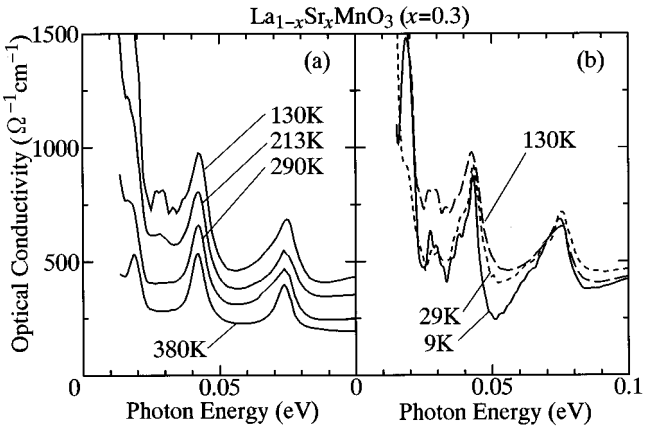

FIG. 9. Low-energy parts of the optical conductivity spectra in $La_{1-x}Sr_xMnO_3$ ($x=0.3$) at 130–380 K (a) and at 9–130 K (b).

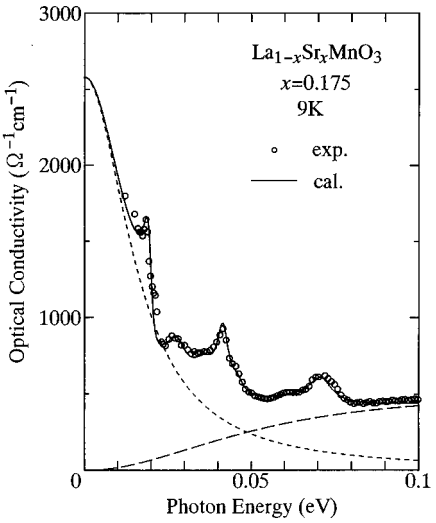

FIG. 10. The parameter-fitted result (a solid line) of the optical conductivity spectrum at 9 K (open circles) in $La_{1-x}Sr_xMnO_3$ ($x=0.175$) using the Drude-Lorentz model (see text). The calculated Drude and incoherent parts are shown by dotted and dashed lines, respectively.

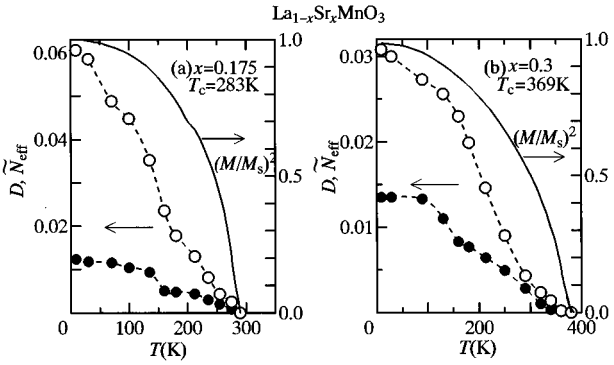

FIG. 11. Temperature dependence of the inner-gap absorption $\tilde{N}_{\rm eff}$ (open circles) and Drude weight D (closed circles) in $La_{1-x}Sr_xMnO_3$ for $x=0.175$ (a) and $x=0.3$ (b) (see text). Broken lines are merely a guide to the eyes. The solid line shows the temperature dependence of square of the normalized ferromagnetic magnetization $(M/M_s)^2$, M_s being the saturated magnetization ($4.0\mu_B$ for $x=0.175$ and $3.5\mu_B$ for $x=0.3$) at the lowest temperature.

respectively. (The remaining part is due to the optical-phonon modes.) We defined the Drude weight D as area of the Drude part.

We may deduce the spectral weight of the inner-gap absorption, i.e., summation of the coherent (Drude) and incoherent parts, which is defined by the following relation:

$$\tilde{N}_{\rm eff}(\omega_c)=\frac{2m}{\pi e^2 N}\int_0^{\omega_c}\tilde{\sigma}(\omega)d\omega. \tag{3}$$

Here N represents the number of formula units (i.e., the number of Mn atoms) per unit volume. For the cutoff energy $\hbar\omega_c$, we choose the energy at which the reduced optical conductivity $\tilde{\sigma}(\omega)$ shows a well-defined minimum, making a distinction between the interband and intraband excitations (see Fig. 6). In Figs. 11(a) and 11(b), we show the temperature dependence of the two parameters D (closed circle) and $\tilde{N}_{\rm eff}$ (open circle) in $x=0.175$ (a) and $x=0.3$ (b), respectively. [Note that $\tilde{N}_{\rm eff}$ for $x=0.3$ excludes the T-independent contribution because of the aforementioned subtraction procedure. For $x=0.3$, the paramagnetic phase above T_c is metallic, and the total spectral weight of the incoherent part should be considered as sum of the T-dependent $\tilde{N}_{\rm eff}$ and the background part (perhaps $\leqslant 0.03$ judging from the original spectrum in Fig. 5).] For reference, we also show the temperature dependence of square of the normalized ferromagnetic magnetization $(M/M_s)^2$ in the figure. (The measurements of M were performed under a magnetic field of 0.5 T.) M_s is the saturated magnetization at the lowest temperature ($\approx 4.0\mu_B$ in $x=0.175$ and $\approx 3.5\mu_B$ in $x=0.3$). The calculation by the dynamical mean-field approximation[29] indicates that the weight of intraband excitations within the lower exchange-split band is proportional to $(M/M_s)^2$. As is clearly seen, the temperature variation of $\tilde{N}_{\rm eff}$ is quite different from that of $(M/M_s)^2$: Even in the lower-temperature region where $(M/M_s)^2$ is almost saturated, $\tilde{N}_{\rm eff}$ keeps on changing, in particular for $x=0.175$. Such a contradiction to the prediction by the simple double-exchange model implies that some large-energy-scale carrier scattering mechanism other than the spin fluctuation may survive down to much lower temperatures than T_c.

Anomalously small Drude weight as estimated by the aforementioned procedure may also be relevant to such a carrier scattering. The Drude weight D is as small as ≈ 0.012 even for the lowest temperature spectra for both $x=0.175$ and 0.3. For $x=0.175$, the Drude weight is $\approx 1/5\tilde{N}_{\rm eff}$. In a simple Drude model, $D\propto n/m^*$, n being the carrier number per Mn site, and m^* effective mass in unit of m_0 (bare mass). Then m^* is estimated to be ≈ 80, provided that the effective carrier density $n\approx 1$ as given by measurement of (ordinary) Hall coefficient.[48] However, such an enormously heavy mass as derived by this simplified interpretation appears to be incompatible with the results of electronic specific heat measurements by Kumagai and Tokura:[49] The conventional low-temperature T-linear specific heat is observed for the metallic phase ($x\geqslant 0.17$) and the coefficient γ is 5–6 mJ/mol K^2, being nearly independent of x. The value is typical of the least-renormalized band mass ($2m_0$–$3m_0$). The behavior is also contrasted by the critically x-dependent mass renormalization as observed in the case of doped Mott insulators, such as $La_{1-x}Sr_xTiO_3$.[50] It is worth noting here that the apparently very small Drude weight against the dominant incoherent-part is quite consistent with the valence-electron photoemission spectra of the relevant manganites in which the unconventionally small spectral weight is barely observed at the Fermi level.[24,51] Nevertheless, these spectroscopic observations cannot be simply related to the other low-energy transport and thermodynamical properties, e.g., in terms of the simple Brinkman-Rice picture.[52] The peculiar behaviors observed in the low-energy optical spectra which cannot be explained by the simple double-exchange model or by the conventional Fermi-liquid picture are summarized as follows:

(1) The low-energy spectra are composed mostly of the incoherent part and lightly (about 20–30 % in fraction) of the Drude response.

(2) The low-energy spectral weight composed of both the incoherent and coherent parts shows the persistent temperature dependence even in the low-temperature region where the conduction electrons (or holes) are almost fully spin polarized.

(3) The small Drude weight arises from neither the heavy effective mass nor the small carrier density.

At present, we have no definite scenario for explanation of all the above observations, yet may speculate about possible origins for the strong carrier scattering. One is to invoke the dynamical Jahn-Teller effect. The persistent Jahn-Teller distortion may result in the formation of small polarons which are barely mobile even at low temperature. The minimal Drude weight, the dominant incoherent part, and their persistent temperature dependence might be explained by this hypothesis, but the seemingly unrenormalized γ might hardly be reconciled. Another possible mechanism may be related to the orbital degree of freedom in the e_g conduction state. The orbital may show the strong correlation and fluctuation even in the almost fully spin-polarized state. As an origin for the anomalous metallic state of $La_{1-x}Sr_xMnO_3$ as observed here, Ishihara, Yamanaka, and Nagaosa[53] recently proposed the concept of an orbital liquid in which the ''ferromagnetic'' correlation of the $d_{x^2-y^2}$ orbitals and the resultant two-dimensional electronic character are enhanced, but can be disordered down to low temperature. The internal consistency and discrepancy among the results of various measurements should be further investigated to unravel the nature of this intriguing metallic state.

V. CONCLUSION

To unravel the electronic structure in $La_{1-x}Sr_xMnO_3$ and its variation with band filling (or hole concentration x) and temperature (or the averaged spin polarization of the conduction holes), we systematically investigated the optical conductivity spectra for single crystals with $x=0.1$ (insulating even below T_c), 0.175 (barely metallic below T_c but semiconducting above T_c), and 0.3 (metallic). For the $x=0.1$ crystal, the spectral intensity is accumulated in the midinfrared region with decrease of temperature below T_c but never comes close to zero energy, reflecting the insulating ground state. A typical energy (0.5 eV) of the midinfrared band is considered as representing the binding energy of the polarons which may arise from the Jahn-Teller or relevant electron-orbital coupling. In the metallic crystals, $x=0.175$ and 0.3, on the other hand, the conductivity spectra show a critically temperature-dependent transfer of the spectral weight from the interband excitation part to the intraband one relating to the exchange-split conduction bands. The energy scale of the spectral weight transfer corresponds to the effective splitting of the spin-polarized conduction band due to the large Hund's-rule coupling energy exceeding the bandwidth; approximately 2 eV for $x=0.175$ and 0.9 eV for $x=0.3$. The observed x-dependent change of the band splitting energy is perhaps ascribed to the increasing p-hole character with x.

The intraband transitions in the metallic phase, which dominate the spectrum up to ≈ 1 eV, is far from the conventional Drude spectrum but should mostly be considered as an incoherent part. In fact, the real Drude part is discernible below 0.04 eV, but with an anomalously small spectral weight (roughly one-fifth of the total intraband spectral weight). The spectral weight of the incoherent plus coherent parts grows with the spin polarization, as expected from the exchange-split band feature. However, the spectral weight keeps on changing in a sufficiently low-temperature region (say below 50 K) in which the spin-polarization (or ferromagnetic magnetization) nearly saturates. These features may indicate the presence of the strong carrier scattering process other than the spin fluctuation being persistent down to low temperature. Such a strong carrier scattering mechanism may also be responsible for the squeezed Drude weight. This is inherently not included in the simple double-exchange model, and is perhaps relevant to the orbital degree of freedom of the e_g spin-polarized electrons (or holes) or to the resultant dynamical Jahn-Teller coupling. The anomalously small Drude weight is simply related neither to heavy carrier mass nor to small carrier density, since the opposite situation has been observed in measurements of electronic specific heat and Hall coefficient. The dynamics of the fully spin-polarized electrons (or holes) with retaining orbital degrees of freedom in the doped perovskite manganites thus gives rise to unconventional metallic phase, the origin of which deserves for a further study.

ACKNOWLEDGMENTS

We acknowledge valuable discussions with N. Furukawa, M. Tachiki, N. Nagaosa, S. Ishihara, and A. J. Millis. We would also like to thank A. Urushibara and A. Asamitsu for the sample preparation and characterization, and K. Kumagai for sharing the specific-heat data prior to publication. The measurements of reflectivity spectra in vacuum ultraviolet region were performed at the INS-SOR, Institute for Solid State Physics, the University of Tokyo. This work was supported in part by a Grant-in-Aid for Scientific Research from the Ministry of Education, Science, Sport and Culture, Japan, and by New Energy and Industrial Technology Development Organization (NEDO).

*Present address: Institute of Materials Science, University of Tsukuba.

[1] G. H. Jonker and J. H. van Santen, Physica **16**, 337 (1950).
[2] G. H. Jonker and J. H. van Santen, Physica **19**, 120 (1953).
[3] E. O. Wollan and W. C. Coehler, Phys. Rev. **100**, 545 (1955).
[4] C. Zener, Phys. Rev. B **82**, 403 (1951).
[5] P. W. Anderson and H. Hasegawa, Phys. Rev. **100**, 675 (1955).
[6] P. -G. de Gennes, Phys. Rev. **118**, 141 (1960).
[7] R. M. Kusters, D. A. Singleton, R. McGreevy, and W. Heyes, Physica B **155**, 362 (1989).
[8] K. Chahara, T. Ohno, M. Kasai, and Y. Kozono, Appl. Phys. Lett. **63**, 1990 (1993).
[9] R. von Helmolt, J. Wecker, B. Holzapfel, L. Schultz, and K. Samwer, Phys. Rev. Lett. **71**, 2331 (1993).

[10] Y. Tokura, A. Urushibara, Y. Moritomo, A. Asamitsu, G. Kido, and N. Furukawa, J. Phys. Soc. Jpn. **63**, 418 (1994).
[11] M. McCormack, S. Jin, T. H. Tiefel, R. M. Fleming, J. M. Phillips, and R. Ramesh, Appl. Phys. Lett. **64**, 3045 (1994).
[12] S. Jin, T. H. Tiefel, M. McCormack, R. A. Fastnacht, R. Ramesh, and L. H. Chen, Science **264**, 413 (1994).
[13] H. L. Ju, C. Kwon, Qi Li, R. H. Greene, and T. Venkatesan, Appl. Phys. Lett. **65**, 2108 (1994).
[14] A. Urushibara, Y. Moritomo, T. Arima, A. Asamitsu, G. Kido, and Y. Tokura, Phys. Rev. B **51**, 14 103 (1995).
[15] Y. Tomioka, A. Asamitsu, Y. Moritomo, H. Kuwahara, and Y. Tokura, Phys. Rev. Lett. **74**, 5108 (1995).
[16] P. Schiffer, A. P. Ramirez, W. Bao, and S.-W. Cheong, Phys. Rev. Lett. **75**, 3336 (1995).
[17] Y. Tomioka, A. Asamitsu, Y. Moritomo, and Y. Tokura, J. Phys. Soc. Jpn. **64**, 3626 (1995).
[18] H. Kuwahara, Y. Tomioka, A. Asamitsu, Y. Moritomo, and Y. Tokura, Science **270**, 961 (1995).
[19] A. Asamitsu, Y. Tomioka, Y. Moritomo, T. Arima, and Y. Tokura, Nature **373**, 407 (1995).
[20] A. Asamitsu, Y. Moritomo, R. Kumai, Y. Tomioka, and Y. Tokura, Phys. Rev. B **54**, 1716 (1996).
[21] H. Y. Hwang, S-W. Cheong, N. P. Ong, and B. Batlogg, Phys. Rev. Lett. **77**, 2041 (1996).
[22] T. Kimura, Y. Tomioka, H. Kuwahara, A. Asamitsu, M. Tamura, and Y. Tokura, Science **274**, 1698 (1996).
[23] T. Arima, Y. Tokura, and J. B. Torrance, Phys. Rev. B **48**, 17 006 (1993).
[24] T. Saitoh, A. E. Bocquet, T. Mizokawa, H. Namatame, A. Fujimori, M. Abbate, Y. Takeda, and M. Takano, Phys. Rev. B **51**, 13 942 (1995).
[25] J. Zaanen, G. A. Sawatzky, and J. W. Allen, Phys. Rev. Lett. **55**, 418 (1985).
[26] K. Kubo and N. Ohata, J. Phys. Soc. Jpn. **33**, 21 (1972).
[27] N. Hamada, H. Sawada, and K. Terakura, in *Spectroscopy of Mott Insulators and Correlation Metals*, edited by A. Fujimori and Y. Tokura (Spinger-Verlag, Berlin, 1995).
[28] N. Furukawa, J. Phys. Soc. Jpn. **64**, 2734 (1995).
[29] N. Furukawa, J. Phys. Soc. Jpn. **64**, 3164 (1995).
[30] Y. Okimoto, T. Katsufuji, T. Ishikawa, A. Urushibara, T. Arima, and Y. Tokura, Phys. Rev. Lett. **75**, 109 (1995).
[31] A. Wold and R. J. Arnott, J. Phys. Chem. Solids **9**, 176 (1959).
[32] H. Kawano, R. Kajimoto, M. Kubota, and H. Yoshizawa, Phys. Rev. B **53**, 14 709 (1996).
[33] To be precise, weak antiferromagnetic peaks are observed in the magnetic neutron scattering up to $x = 0.15$, suggesting canted spin structure (Ref. 32).
[34] C. M. Varma (unpublished).
[35] A. J. Millis, P. B. Littlewood, and B. I. Shraiman, Phys. Rev. Lett. **74**, 5144 (1995).
[36] T. Arima and Y. Tokura, J. Phys. Soc. Jpn. **64**, 2488 (1995).
[37] S. Yamaguchi, Y. Okimoto, and Y. Tokura (unpublished).
[38] J. B. Torrance, P. Lacorre, C. Asavaroengchai, and R. M. Metzger, Physica C **182**, 351 (1991).
[39] Y. Taguchi, Y. Tokura, T. Arima, and F. Inaba, Phys. Rev. B **48**, 511 (1993).
[40] F. Inaba, T. Arima, T. Ishikawa, T. Katsufuji, and Y. Tokura, Phys. Rev. B **52**, 2221 (1995).
[41] S. Uchida, T. Ido, H. Takagi, T. Arima, Y. Tokura, and S. Tajima, Phys. Rev. B **43**, 7942 (1991).
[42] T. Katsufuji, Y. Okimoto, and Y. Tokura, Phys. Rev. Lett. **75**, 3497 (1995).
[43] Y. Okimoto, T. Katsufuji, Y. Okada, T. Arima, and Y. Tokura, Phys. Rev. B **51**, 9581 (1995).
[44] A. J. Millis, R. Mueller, and Boris I. Shraiman, Phys. Rev. B **54**, 5405 (1996).
[45] H. Roder, Jun Zang, and A. R. Bishop, Phys. Rev. Lett. **76**, 1356 (1996).
[46] For example, K. Tamasaku, Y. Nakamura, and S. Uchida, Phys. Rev. Lett. **69**, 1445, (1992); C. C. Homes, T. Timusk, R. Liang, D. A. Bonn, and W. N. Hardy, *ibid.* **71**, 1645 (1993).
[47] We adopted a simple Lorentzian form as the dielectric function for the incoherent part, but used an asymmetric Larenzian for the optical-phonon parts to obtain better fitting.
[48] A. Asamitsu, Y. Moritomo, and Y. Tokura (unpublished).
[49] K. Kumagai and Y. Tokura (unpublished).
[50] Y. Tokura, Y. Taguchi, Y. Okada, Y. Fujishima, T. Arima, K. Kumagai, and Y. Iye, Phys. Rev. Lett. **70**, 2120 (1993).
[51] J.-H. Park, C. T. Chen, S-W. Cheong, W. Bao, G. Meigs, V. Chakarian, and Y. U. Idzerda, Phys. Rev. Lett. **76**, 4215 (1996).
[52] W. F. Brinkman and T. M. Rice, Phys. Rev. B **2**, 4302 (1970).
[53] S. Ishihara, M. Yamanaka, and N. Nagaosa (unpublished).